Table 1 Clinical features of *Kv*DMR-LOM patients with monolocus methylation defect and those with multilocus methylation defects

	Methylation defect		
	Monolocus	Multilocus	*P* value
Sex			0.22
Male	15	5	
Female	13	9	
Average age of patients	3.3	2.4	0.098[a]
Average age of parents			
Father	31.8	33.8	0.93[a]
Mother	31.8	30.3	0.37[a]
Assisted reproduction technology	3/19 (20%) (AIH 2, OS 1)	2/8 (29%) (ICSI 1, OS 1)	0.47
Standard deviation of average birth weight	+1.9	+2.0	0.58[a]
Overgrowth	21/28 (75%)	9/13 (69%)	0.78
Abdominal wall defect	22/29 (76%)	12/13 (92%)	0.21
Macroglossia	29/29 (100%)	12/12 (100%)	0.60
Hypoglycemia	14/27 (52%)	5/12 (42%)	0.41
Ear pits and creases	19/27 (70.4%)	8/12 (67%)	0.73
Nevus flammeus	9/26 (35%)	4/10 (40%)	0.53
Hemihypertrophy	6/27 (22%)	6/13 (46%)	0.12
Renal anomaly	2/26 (8%)	0/11 (0%)	0.49
Renal enlargement	6/28 (21%)	1/13 (8%)	0.27
Adrenal enlargement	1/27 (4%)	0/11 (0%)	0.71
Hepatomegaly	5/29 (17%)	2/12 (17%)	0.67
Splenomegaly	6/29 (21%)	2/12 (17%)	0.57
Abnormal external genitalia	2/28 (7%)	0/12 (0%)	0.49
Increased bone age	2/15 (13%)	0/3 (0%)	0.69
Cardiac anomaly	2/23 (9%)	0/11 (0%)	0.82
Developmental retardation	6/22 (27%)	0/9 (0%)	0.10
Childhood tumor	5/26 (19%)	0/11 (0%)	0.15

AIH, artificial insemination by husband; ICSI, intracytoplasmic sperm injection; LOM, loss of methylation; OS, ovulation stimulation.

[a]Mann–Whitney *U*-test. Fisher's exact test was used for other analyses.

64).[11,12] In addition, we found that 30.0% of *H19*DMR-GOM patients showed MMDs, which is surprising considering that no MMDs were found in two previous reports in which 10 and 16 DMRs were analyzed.[8,11] These data suggest that the greater the number of DMRs analyzed, the higher the frequency of MMDs observed. In future, all DMRs in the genome should be analyzed to understand the precise frequency of MMDs, which DMRs become preferentially aberrantly methylated, and the mechanism by which MMDs occur.

In both *Kv*DMR1-LOM patients and *H19*DMR-GOM patients, we found MMDs in which not only LOM but also GOM were seen. We also found that both matDMRs and patDMRs were aberrantly methylated in both patient groups. It is noteworthy that matDMRs, probably gametic maternally methylated DMRs, were more susceptible to aberrant methylation than patDMRs in *Kv*DMR1-LOM patients, although no particular parent-based pattern of aberrant methylation has been reported previously.[12] This suggests that gametic maternally methylated DMRs are vulnerable to DNA demethylation during the preimplantation stage of early embryogenesis when *Kv*DMR1-LOM occurs.

Although it has not been reported that aberrant methylation of the corresponding DMR affects imprinted gene expression in MMD patients, we found biallelic expression of three imprinted genes (*ZDBF2*, *FAM50B*, and *GNAS1A*) to be associated with the aberrant methylation of their respective DMRs. Because biallelic expression increased the total expression levels of *ZDBF2* and *FAM50B*, we expect that had we measured the expression levels of *GNAS1A*, we would have observed an increase. Therefore, alteration of gene expression levels due to MMDs might affect the phenotype; however, clinical features between MMDs and monolocus methylation defects were not different in our study. This lack of difference has been previously reported,[7,9,10,13] although a few groups have reported a

difference in clinical features.[8,11,12] Two reasons for this similarity in terms of clinical features could be suggested. First, the mosaic ratio might be different in each organ. Because aberrant methylation was generally partial, it would occur after fertilization, and the patients would be mosaic. A high mosaic ratio would be a critical factor in the emergence of a distinct phenotype in BWS patients with monolocus methylation defects. Second, the imprinted locus at 11p15 might be epidominant over other imprinted loci because all MMD patients were clinically diagnosed as BWS.

Regarding the causative factor(s) for MMD, we could not find any pathological variation in any aberrantly methylated DMR, including *Kv*DMR1, suggesting that *cis*-acting variations of each specific DMR itself were not involved in the genesis of MMDs. On the other hand, the involvement of *trans*-acting factors has been advocated in other reports because mutations of *ZFP57* (which are required for the postfertilization maintenance of maternal and paternal methylation imprinting at multiple loci) have been found in transient neonatal diabetes mellitus type 1 patients with multilocus hypomethylation.[32] Mutations of *NLRP2* were also identified in a BWS patient with *Kv*DMR1-LOM and *MEST*-LOM in a family with complex consanguinity and in a Silver–Russell syndrome patient with multilocus hypomethylation.[12,33] In addition, TRIM28, NLRP7, KHDC3L, and DNMT3L have been considered to be candidate *trans*-acting factors. However, no mutations in any of these candidates or other genes, such as *DNMT1*, *DNMT3A*, and *DNMT3B*, were found in our BWS patients with MMDs, as determined by exome sequencing (K. Sasaki and K. Hata, personal communication). Recently, Lorthongpanich et al.[34] reported that the absence of maternal *Trim28* until zygotic gene activation at the two-cell late stage caused mosaicism of MMDs randomly, suggesting that insufficient expression of the candidate gene(s) at very early embryogenesis is an important event in the generation of MMDs in human imprinted diseases. Whole-genome sequencing and whole-genome bisulfite sequencing, including the regulatory regions of the candidate genes, and transcriptome analysis in early embryogenesis would be useful to identify the cause(s) of MMDs.

In our *H19*DMR-GOM patients, we also found GOM of *IGF2*-DMR0 and *IGF2*-DMR2 to be associated with GOM of *H19*DMR and *H19promoter* DMR, in agreement with previous reports.[22,35,36] Two patients showed simultaneous GOM at both *IGF2*-DMRs. Because *Igf2*-DMRs were established at the postimplantation stage under the control of *H19*DMR in mice,[37] GOM of *IGF2*-DMRs in BWS is likely to occur at the same stage. Although the function of *IGF2*-DMR0 is still unknown, methylated *Igf2*-DMR2 plays a role in transcription initiation of *Igf2* in mice.[38] GOM of the DMRs might change the high-order chromatin structure of the maternal allele and increase the expression of *IGF2* in cooperation with *H19*DMR-GOM in BWS patients.

In conclusion, our comprehensive and quantitative methylation analysis of multiple imprinted DMRs revealed several new findings: (i) matDMRs, probably gametic maternally methylated DMRs, are more susceptible to aberrant methylation during the preimplantation stage, when *Kv*DMR1-LOM occurs; (ii) aberrant methylation indeed alters imprinted gene expression; and (iii) *cis*-acting pathological variations of each DMR are not involved in the MMDs analyzed. Moreover, our study confirmed the simultaneous aberrant hypermethylation of *IGF2*-DMR0 and/or -DMR2 with isolated *H19*DMR-GOM. These findings may help us to understand the molecular mechanisms and pathophysiological features of MMDs.

SUPPLEMENTARY MATERIAL

Supplementary material is linked in the online version of the paper at http://www.nature.com/gim.

ACKNOWLEDGMENTS

We thank all the participants and their families who provided samples and all the doctors who referred patients to us. This study was supported, in part, by a Grant for Research on Intractable Diseases from the Ministry of Health, Labor, and Welfare; a Grant for Child Health and Development from the National Center for Child Health and Development; a Grant-in-Aid for Challenging Exploratory Research; and a Grant-in-Aid for Scientific Research (C) from the Japan Society for the Promotion of Science.

DISCLOSURE

The authors declare no conflict of interest.

REFERENCES

1. Abramowitz LK, Bartolomei MS. Genomic imprinting: recognition and marking of imprinted loci. *Curr Opin Genet Dev* 2012;22:72–78.
2. Tomizawa S, Sasaki H. Genomic imprinting and its relevance to congenital disease, infertility, molar pregnancy and induced pluripotent stem cell. *J Hum Genet* 2012;57:84–91.
3. Weksberg R, Shuman C, Beckwith JB. Beckwith-Wiedemann syndrome. *Eur J Hum Genet* 2010;18:8–14.
4. Choufani S, Shuman C, Weksberg R. Beckwith-Wiedemann syndrome. *Am J Med Genet C Semin Med Genet* 2010;154C:343–354.
5. Soejima H, Higashimoto K. Epigenetic and genetic alterations of the imprinting disorder Beckwith-Wiedemann syndrome and related disorders. *J Hum Genet* 2013;58:402–409.
6. Mackay DJ, Boonen SE, Clayton-Smith J, et al. A maternal hypomethylation syndrome presenting as transient neonatal diabetes mellitus. *Hum Genet* 2006;120:262–269.
7. Rossignol S, Steunou V, Chalas C, et al. The epigenetic imprinting defect of patients with Beckwith-Wiedemann syndrome born after assisted reproductive technology is not restricted to the 11p15 region. *J Med Genet* 2006;43:902–907.
8. Bliek J, Verde G, Callaway J, et al. Hypomethylation at multiple maternally methylated imprinted regions including PLAGL1 and GNAS loci in Beckwith-Wiedemann syndrome. *Eur J Hum Genet* 2009;17:611–619.
9. Azzi S, Rossignol S, Steunou V, et al. Multilocus methylation analysis in a large cohort of 11p15-related foetal growth disorders (Russell Silver and Beckwith Wiedemann syndromes) reveals simultaneous loss of methylation at paternal and maternal imprinted loci. *Hum Mol Genet* 2009;18:4724–4733.
10. Lim D, Bowdin SC, Tee L, et al. Clinical and molecular genetic features of Beckwith-Wiedemann syndrome associated with assisted reproductive technologies. *Hum Reprod* 2009;24:741–747.
11. Poole RL, Docherty LE, Al Sayegh A, et al.; International Clinical Imprinting Consortium. Targeted methylation testing of a patient cohort broadens the epigenetic and clinical description of imprinting disorders. *Am J Med Genet A* 2013;161:2174–2182.
12. Court F, Martin-Trujillo A, Romanelli V, et al. Genome-wide allelic methylation analysis reveals disease-specific susceptibility to multiple methylation defects in imprinting syndromes. *Hum Mutat* 2013;34:595–602.

13. Tee L, Lim DH, Dias RP, et al. Epimutation profiling in Beckwith-Wiedemann syndrome: relationship with assisted reproductive technology. *Clin Epigenetics* 2013;5:23.
14. DeBaun MR, Tucker MA. Risk of cancer during the first four years of life in children from The Beckwith-Wiedemann Syndrome Registry. *J Pediatr* 1998;132(3 Pt 1):398–400.
15. Soejima H, Nakagawachi T, Zhao W, et al. Silencing of imprinted CDKN1C gene expression is associated with loss of CpG and histone H3 lysine 9 methylation at DMR-LIT1 in esophageal cancer. *Oncogene* 2004;23:4380–4388.
16. Higashimoto K, Nakabayashi K, Yatsuki H, et al. Aberrant methylation of H19-DMR acquired after implantation was dissimilar in soma versus placenta of patients with Beckwith-Wiedemann syndrome. *Am J Med Genet A* 2012;158A:1670–1675.
17. Yatsuki H, Higashimoto K, Jozaki K, et al. Novel mutations of CDKN1C in Japanese patients with Beckwith-Wiedemann syndrome. *Genes & Genomics* 2013;35:141–147.
18. Higashimoto K, Jozaki K, Kosho T, et al. A novel de novo point mutation of the OCT-binding site in the IGF2/H19-imprinting control region in a Beckwith-Wiedemann syndrome patient. *Clin Genet* 2013; e-pub ahead of print 8 November 2013.
19. Ehrich M, Nelson MR, Stanssens P, et al. Quantitative high-throughput analysis of DNA methylation patterns by base-specific cleavage and mass spectrometry. *Proc Natl Acad Sci USA* 2005;102:15785–15790.
20. Rumbajan JM, Maeda T, Souzaki R, et al. Comprehensive analyses of imprinted differentially methylated regions reveal epigenetic and genetic characteristics in hepatoblastoma. *BMC Cancer* 2013;13:608.
21. Cui H, Onyango P, Brandenburg S, Wu Y, Hsieh CL, Feinberg AP. Loss of imprinting in colorectal cancer linked to hypomethylation of H19 and IGF2. *Cancer Res* 2002;62:6442–6446.
22. Murrell A, Ito Y, Verde G, et al. Distinct methylation changes at the IGF2-H19 locus in congenital growth disorders and cancer. *PLoS One* 2008;3: e1849.
23. Woodfine K, Huddleston JE, Murrell A. Quantitative analysis of DNA methylation at all human imprinted regions reveals preservation of epigenetic stability in adult somatic tissue. *Epigenetics Chromatin* 2011;4:1.
24. Reik W, Maher ER. Imprinting in clusters: lessons from Beckwith-Wiedemann syndrome. *Trends Genet* 1997;13:330–334.
25. Kobayashi H, Yamada K, Morita S, et al. Identification of the mouse paternally expressed imprinted gene Zdbf2 on chromosome 1 and its imprinted human homolog ZDBF2 on chromosome 2. *Genomics* 2009;93:461–472.
26. Nakabayashi K, Trujillo AM, Tayama C, et al. Methylation screening of reciprocal genome-wide UPDs identifies novel human-specific imprinted genes. *Hum Mol Genet* 2011;20:3188–3197.
27. Liu J, Litman D, Rosenberg MJ, Yu S, Biesecker LG, Weinstein LS. A GNAS1 imprinting defect in pseudohypoparathyroidism type IB. *J Clin Invest* 2000;106:1167–1174.
28. Demars J, Shmela ME, Rossignol S, et al. Analysis of the IGF2/H19 imprinting control region uncovers new genetic defects, including mutations of OCT-binding sequences, in patients with 11p15 fetal growth disorders. *Hum Mol Genet* 2010;19:803–814.
29. Weksberg R, Shuman C, Caluseriu O, et al. Discordant KCNQ1OT1 imprinting in sets of monozygotic twins discordant for Beckwith-Wiedemann syndrome. *Hum Mol Genet* 2002;11:1317–1325.
30. Tost J, Dunker J, Gut IG. Analysis and quantification of multiple methylation variable positions in CpG islands by Pyrosequencing. *Biotechniques* 2003;35:152–156.
31. Claus R, Wilop S, Hielscher T, et al. A systematic comparison of quantitative high-resolution DNA methylation analysis and methylation-specific PCR. *Epigenetics* 2012;7:772–780.
32. Mackay DJ, Callaway JL, Marks SM, et al. Hypomethylation of multiple imprinted loci in individuals with transient neonatal diabetes is associated with mutations in ZFP57. *Nat Genet* 2008;40:949–951.
33. Meyer E, Lim D, Pasha S, et al. Germline mutation in NLRP2 (NALP2) in a familial imprinting disorder (Beckwith-Wiedemann Syndrome). *PLoS Genet* 2009;5:e1000423.
34. Lorthongpanich C, Cheow LF, Balu S, et al. Single-cell DNA-methylation analysis reveals epigenetic chimerism in preimplantation embryos. *Science* 2013;341:1110–1112.
35. Reik W, Brown KW, Schneid H, Le Bouc Y, Bickmore W, Maher ER. Imprinting mutations in the Beckwith-Wiedemann syndrome suggested by altered imprinting pattern in the IGF2-H19 domain. *Hum Mol Genet* 1995;4:2379–2385.
36. Sparago A, Russo S, Cerrato F, et al. Mechanisms causing imprinting defects in familial Beckwith-Wiedemann syndrome with Wilms' tumour. *Hum Mol Genet* 2007;16:254–264.
37. Lopes S, Lewis A, Hajkova P, et al. Epigenetic modifications in an imprinting cluster are controlled by a hierarchy of DMRs suggesting long-range chromatin interactions. *Hum Mol Genet* 2003;12:295–305.
38. Murrell A, Heeson S, Bowden L, et al. An intragenic methylated region in the imprinted Igf2 gene augments transcription. *EMBO Rep* 2001;2:1101–1106.

PEDIATRICS INTERNATIONAL Official Journal of the Japan Pediatric Society

Fibroadenoma in Beckwith–Wiedemann syndrome with paternal uniparental disomy of chromosome 11p15.5

Yuichi Takama,[1,3] Akio Kubota,[1] Masahiro Nakayama,[2] Ken Higashimoto,[4] Kosuke Jozaki[4] and Hidenobu Soejima[4]

Departments of [1]Pediatric Surgery and [2]Pathology, Osaka Medical Center and Research for Maternal and Child Health, [3]Department of Pediatric Surgery, Osaka City General Hospital, Osaka and [4]Division of Molecular Genetics and Epigenetics, Department of Biomolecular Sciences, Faculty of Medicine, Saga University, Saga, Japan

Abstract Herein is described a case of breast fibroadenomas in a 16-year-old girl with Beckwith–Wiedemann syndrome (BWS) and uniparental disomy (UPD) of chromosome 11p15.5. She was clinically diagnosed with BWS and direct closure was performed for an omphalocele at birth. Subtotal and 90% pancreatectomy were performed for nesidioblastosis at the ages 2 months and 8 years, respectively. Bilateral multiple breast fibroadenomas were noted at the age of 16 and 17 years. In this case, paternal UPD of chromosome 11p15.5 was identified on microsatellite marker analysis. The relevant imprinted chromosomal region in BWS is 11p15.5, and UPD of chromosome 11p15 is a risk factor for BWS-associated tumorigenicity. Chromosome 11p15.5 consists of imprinting domains of IGF2, the expression of which is associated with the tumorigenesis of various breast cancers. This case suggests that fibroadenomas occurred in association with BWS.

Key words 11p15, Beckwith–Wiedemann syndrome, breast tumor, fibroadenoma, uniparental disomy.

Beckwith–Wiedemann syndrome (BWS) is an overgrowth disorder with a potentiality for various embryonal tumors, such as Wilms tumor, hepatoblastoma, and a variety of other malignant and benign tumors.[1,2] BWS is caused by various epigenetic or genetic alterations associated with chromosome 11p15, such as uniparental disomy (UPD).[1] We report a case of breast fibroadenomas and ovarian adenofibroma in a 16-year-old girl with BWS and UPD of chromosome 11p15.5, and discuss the relationship between fibroadenoma, which is relatively common in adolescents, and BWS and paternal UPD on chromosome 11p15.5.

Case report

The patient was a 16-year-old girl who was diagnosed with BWS at birth based on the following genetic characteristics: macrosomia, omphalocele, macroglossia, and hypoglycemia. Her birthweight was 4254 g. Direct closure was performed for the omphalocele immediately after birth.

At the age of 2 months, exploratory laparotomy was performed due to extremely high serum α-fetoprotein and intra-abdominal cystic lesion, which found a hepatic cyst and the tumor-forming type of nesidioblastosis.[2] Resection of the hepatic cyst and subtotal pancreatectomy were performed. Because the patient experienced hypoglycemic episodes 2–3 times per year, 90% pancreatectomy was again performed for nesidioblastosis at the age of 8 years.[2] Thereafter, she had no further hypoglycemic episodes. We previously reported on that course.[2]

At the age of 16 years, a right breast tumor was noticed, which grew over time. Extirpation was performed and histology confirmed breast fibroadenoma (Fig. 1a). Three months after extirpation of the breast tumor, the patient presented with lower abdominal distention; ultrasonography indicated that this was caused by an ovarian solid and cystic mass. The cystic lesion was resected, and histology confirmed adenofibroma (Fig. 1b).

At the age of 17 years, bilateral multiple tumors of the breasts were detected on follow-up ultrasonography, which were confirmed to be fibroadenomas on needle biopsy. The patient received no further intervention and has been followed up for 6 years.

Previously, we studied chromosome 11p for identification of the disorder using G banding, but no anomaly was detected. Recently, re-evaluation of chromosome 11p using microsatellite marker analysis indicated paternal UPD of chromosome 11p15.5. Although we analyzed three microsatellite markers, D11S2362, D11S1318 and TH01, only one microsatellite marker, D11S1318, provided useful information about the patient. The percentage mosaicism of paternal UPD in the patient's DNA was 98% and 69% from peripheral blood and saliva, respectively (Fig. 2).

Discussion

Classically, BWS is diagnosed based on clinical features such as abdominal wall defects, macroglossia, and macrosomia.[1,2] BWS is the most common congenital overgrowth syndrome involving tumor predisposition and has a strong correlation with embryonal tumors such as Wilms tumor, hepatoblastoma, neuroblastoma, adrenocortical carcinoma, and a variety of other malignant and benign tumors.[1,2] The overall risk of tumor development has been

Correspondence: Akio Kubota, MD PhD, Department of Pediatric Surgery, Osaka Medical Center and Research for Maternal and Child Health, 840 Murodocho, Izumi, Osaka 594-1101, Japan. Email: kubota@wakayama-med.ac.jp

Received 9 August 2013; revised 16 March 2014; Accepted date: 7 April 2014.
doi: 10.1111/ped.12406

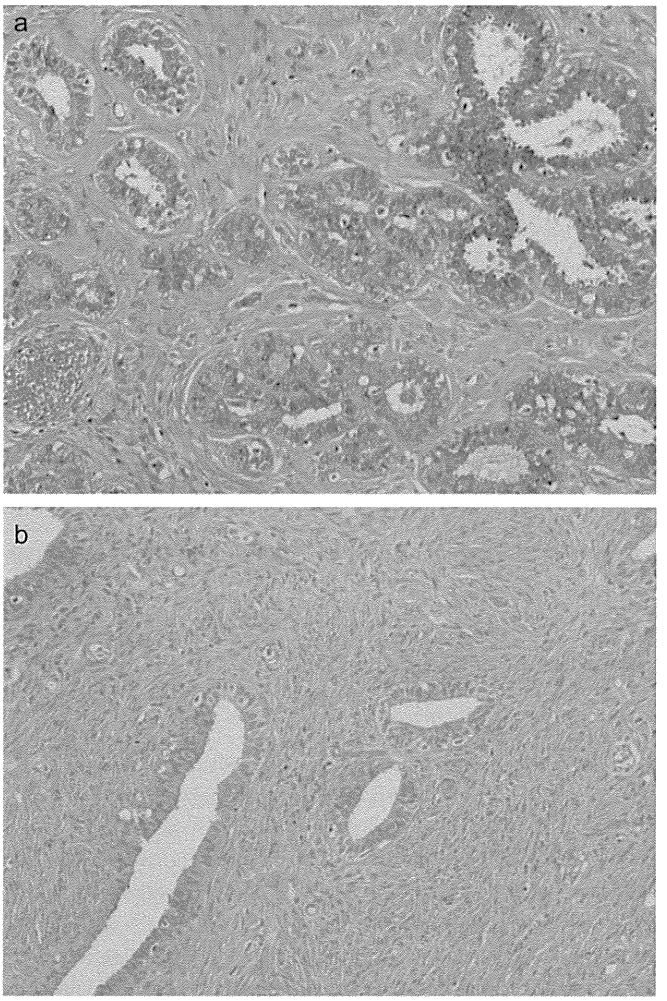

Fig. 1 (a) Many ductular structures are visible, surrounded by moderately cellular stromal connective tissue. The stromal nuclei show little pleomorphism with infrequent mitosis. Breast fibroadenomas were diagnosed. (b) Proliferation of stromal cells and ductules is observed. Ductules are lined with ciliated high columnar epithelial cells. An ovarian adenofibroma was diagnosed.

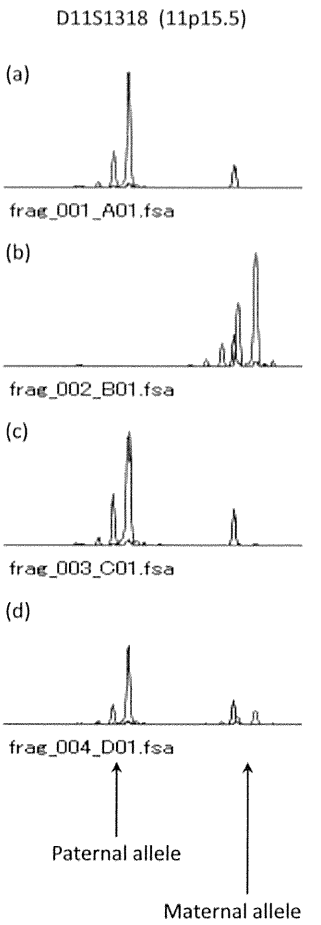

Fig. 2 Microsatellite marker analysis. (a) Father; (b) mother; (c,d) patient DNA (c, peripheral blood; d, saliva). A microsatellite marker, *D11S1318*, from 11p15.5 was amplified and separated on electrophoresis using an Applied Biosystems 3130 genetic analyzer (Applied Biosystems, CA, USA); data were quantitatively analyzed using the GeneMapper software. The percentage mosaicism of paternal UPD was calculated as follows: % mosaicism = $(k - 1)/(k + 1) \times 100$, where k is the ratio of the peak height of the paternal to maternal alleles of the sample. The percentage mosaicism of paternal UPD in the patient's DNA was 98% and 69% from (c) peripheral blood and (d) saliva, respectively.

estimated at 7.5%.[1] Although there are no absolute unified criteria for the clinical diagnosis of BWS, the following criteria are generally accepted: presence of at least three major findings, or two major findings and one minor finding.[1] Major findings associated with BWS include abdominal wall defect, macroglossia, macrosomia, anterior ear lobe creases and/or posterior helical pits, visceromegaly intra-abdominal organ, embryonal tumor, hemihyperplasia, cytomegaly of adrenal fetal cortex, renal abnormalities, positive family history of BWS and cleft palate.[1] Minor findings include neonatal hypoglycemia, nevus flammeus, cardiac anomaly, diastasis recti, advanced bone age and pregnancy-related findings such as polyhydramnios, enlarged placenta and thickened umbilical cord.[1] The relevant imprinted chromosomal region in BWS is 11p15.5. Recently, with the development of molecular genetic analysis, several causative alterations in this region have been identified for sporadic cases of BWS. Paternal UPD of chromosome 11p15 is one such alteration and is found in 20% of BWS patients.[1] UPD occurs when an individual receives both copies of a chromosome or part of a chromosome from one parent. UPD can occur as a random event during the formation of egg cells or sperm cells, or may occur in early fetal development. Non-mosaic genome-wide paternal UPD, however, is known to be lethal.[3] Therefore, BWS patients with paternal UPD are mosaic for paternal UPD cells and normal biparental cells.[1] This indicates that somatic recombination occurs in the post-fertilization stage in BWS patients.[1] UPD of chromosome 11p15 is a reported risk factor for BWS-associated tumorigenicity.[1] The tumor risk for BWS patients with paternal UPD is estimated to be ≥25%.[1] In the present case, embryonal tumors did not develop, although multiple and recurrent fibroadenomas developed.

Although a fibroadenoma is a benign tumor that is relatively common in adolescents, a suspected correlation between BWS

and breast tumors is reported.[4–8] Seven cases, including the present one, of breast fibroadenomas probably associated with BWS have been reported in the literature (Table 1).[5–8] Patient age ranged from infancy, in one case,[4] to adolescence, in six cases.[3,5–8] Four of the seven patients presented with BWS-associated tumor lesions: three presented with Wilms tumors, adrenocortical carcinoma, adrenal pheochromocytoma, hamartoma of the liver, nesidioblastosis, and steroid cell tumor of ovary, whereas the current patient presented with nesidioblastosis, hepatic cyst, and ovarian adenofibroma.[3,5,7]

The chromosomal disorder was not detected in one of the seven patients, and was not mentioned in four of the seven patients. In the present case, paternal UPD of chromosome 11p15 was diagnosed on microsatellite marker analysis. Gogiel *et al.* reported that a 19-year-old woman with BWS, who was diagnosed as a carrier of a mosaic paternal UPD of chromosome 11p15, presented with fibroadenoma.[3] A BWS-associated chromosomal disorder of paternal UPD of chromosome 11p15 has been detected in two cases, including the present case of fibroadenoma with BWS.[3] Earlier in the present case, we used G banding for the detection of a chromosomal disorder on chromosome 11p, but no such disorder was detected using this method. Instead we identified the chromosomal disorder using microsatellite marker analysis. Microsatellites are tandem repeated nucleotide sequences. Individuals typically have two alleles per microsatellite. If the number of repeats for one allele is different from that of the other, two separate bands would be visible. If, however, the individual has a genetic deletion that includes the region containing the microsatellite, only one band would be visible. In the present case, only one band of paternal allele in chromosome 11p15.5 was amplified in the patient's DNA from peripheral blood and saliva (Fig. 2). This analysis indicated paternal UPD of chromosome 11p15.5. Early diagnosis of BWS is important because BWS patients have a predisposition to various tumors such as Wilms tumor, hepatoblastoma, and a variety of other malignant and benign tumors.[1] Therefore, we emphasize the need for additional molecular testing such as microsatellite marker analysis for the diagnosis of BWS if no chromosomal disorder has been detected by G banding.

In this case, we studied DNA only from the peripheral blood and saliva sample and not from the fibroadenoma tissue sample because of degradation of the sample tissue. Therefore, we could not conclude that paternal UPD of chromosome 11p15.5 was identified from the DNA of the fibroadenoma tissue sample. Gogiel *et al.* reported that analysis of breast tumor tissue DNA showed the same paternal UPD pattern as DNA from peripheral blood.[3] Thus, in the present case we could not confirm whether the association of fibroadenoma with BWS in this case was absolute or incidental. There is, however, a high probability of the association because of the unusual presentation of bilateral and multiple breast fibroadenomas, the coexistence of an ovarian adenofibroma, and the identification of paternal UPD of chromosome 11p15.5. In BWS patients, several mechanisms lead to an increased expression of *IGF2*.[1] BWS was one of the first syn-

Table 1 Reported cases of breast fibroadenoma associated with BWS

First author, year	Sex	Breast tumors	Other tumors	Chromosomal disorder	Hypertrophy
Müller, 1978[5]	F	14 years old: FA of right breast	3 years old: Wilms tumor 7 years old: Adrenocortical carcinoma	Not mentioned	Left leg right part of tongue
Raine, 1979[4]	F	7 months old: FA of left breast 17 months old: Recurrence FA	None	Not mentioned	Right leg
Labrune, 1988[6]	F	13 years old: FA of right breast 14 years old: Recurrence FA	None	Normal	Right side
Bemurat, 2002[7]	F	14 years old: FA of bilateral breast	20 years old: Adrenal pheochromocytoma	Not mentioned	Not mentioned
Poh, 2010[8]	F	12 years old: FA of left breast	None	Not mentioned	Right side
Gogiel, 2013[3]	F	18 years old: FA of breast	1 month old: Hamartoma of liver 2 months old: Nesidioblastosis 14 years old: Steroid cell tumor of ovary	11p15.5 paternal UPD	Left side
Present case	F	16 years old: FA of right breast 17 years old: Recurrence of bilateral breast	At birth: Nesidioblastosis 16 years old: Adenofibroma of left ovary	11p15.5 paternal UPD	None

BWS-associated chromosomal disorder of paternal UPD of chromosome 11p15 was detected in two cases, including the present case of fibroadenoma with BWS. BWS, Beckwith–Wiedemann syndrome; FA, fibroadenoma; UPD, uniparental disomy.

dromes in which IGF2 expression was linked to a growth disorder, in addition to its association with the tumorigenesis of various breast cancers.[9,10] Sawyer *et al.* reported that extensive IGF2 overexpression was found in the majority of fibroadenomas.[11] The present case suggests that the development of multiple and recurrent fibroadenomas is associated with BWS-associated UPD of chromosome 11p15.5. We believe that the present case shows a strong correlation between BWS and fibroadenomas.

Conclusion

We encountered a case of multiple and recurrent breast fibroadenomas and an ovarian adenofibroma associated with BWS in a patient diagnosed with paternal UPD of chromosome 11p15.5. Microsatellite marker analysis was useful to diagnose the case, which could not be diagnosed as BWS on G banding. BWS with paternal UPD of chromosome 11p15.5 presents not only as embryonal tumors but also as various benign and malignant tumors. Therefore, early diagnosis of BWS on molecular testing is helpful in screening for tumorigenesis.

References

1 Soejima H, Higashimoto K. Epigenetic and genetic alterations of the imprinting disorder Beckwith-Wiedemann syndrome and related disorders. *J. Hum. Genet.* 2013; **58**: 402–9.
2 Kubota A, Yonekura T, Usui N *et al.* Two cases of persistent hyperinsulinemic hypoglycemia that showed spontaneous regression and maturation of the Langerhans islets. *J. Pediatr. Surg.* 2000; **35**: 1661–2.
3 Gogiel M, Begemann M, Spengler S *et al.* Genome-wide paternal uniparental disomy mosaicism in a woman with Beckwith-Wiedemann syndrome and ovarian steroid cell tumour. *Eur. J. Hum. Genet.* 2013; **21**: 788–91.
4 Raine PA, Noblett HR, Houghton-Allen BW, Campbell PE. Breast fibroadenoma and cardiac anomaly associated with EMG (Beckwith-Wiedemann) syndrome. *J. Pediatr.* 1979; **94**: 633–4.
5 Muller S, Gadner H, Weber B, Vogel M, Riehm H. Wilms' tumor and adrenocortical carcinoma with hemihypertrophy and hamartomas. *Eur. J. Pediatr.* 1978; **127**: 219–26.
6 Labrune B, Latrobe M, Benichou JJ, Robin M, May A. Neonatal hyperinsulinism, congenital corporeal hemihypertrophy, tumor of the breast in adolescence. *Arch. Fr. Pediatr.* 1988; **45**: 413–15.
7 Bemurat L, Gosse P, Ballanger P *et al.* Successful laparoscopic operation of bilateral pheochromocytoma in a patient with Beckwith-Wiedemann syndrome. *J. Hum. Hypertens.* 2002; **16**: 281–4.
8 Poh MM, Ballard TN, Jason Wendel J. Beckwith-Wiedemann syndrome and juvenile fibroadenoma: A case report. *Ann. Plast. Surg.* 2010; **64**: 803–6.
9 Bergman D, Halje M, Nordin M, Engstrom W. Insulin-like growth factor 2 in development and disease: A mini-review. *Gerontology* 2013; **59**: 240–49.
10 Gebeshuber CA, Martinez J. miR-100 suppresses IGF2 and inhibits breast tumorigenesis by interfering with proliferation and survival signaling. *Oncogene* 2012; **32**: 3306–10.
11 Sawyer EJ, Hanby AM, Poulsom R *et al.* Beta-catenin abnormalities and associated insulin-like growth factor overexpression are important in phyllodes tumours and fibroadenomas of the breast. *J. Pathol.* 2003; **200**: 627–32.

Cyclic fluctuation of blood pressure in neonatal neuroblastoma

Jun Fujishiro,[1] Masahiko Sugiyama,[1] Tetsuya Ishimaru,[1] Chizue Uotani,[1] Shinya Tsuchida,[2] Naoto Takahashi,[2] Ryosuke Shiozawa,[2] Junko Takita[2] and Tadashi Iwanaka[1]

Departments of [1]Pediatric Surgery and [2]Pediatrics, Faculty of Medicine, the University of Tokyo, Tokyo, Japan

Abstract Herein is described a case of neonatal neuroblastoma with cyclic blood pressure fluctuation and elevated catecholamines. The fluctuations stabilized after treatment with α-adrenergic blocker and the perioperative course was uneventful. The possibility of catecholamine-related symptoms including hypertension, heart failure, and blood pressure fluctuations should be considered in the treatment for neuroblastoma; if they are present, treatment with α-blockers is effective.

Key words catecholamine, cyclic fluctuation, hypertension, neuroblastoma, α-adrenergic blocker.

Although elevated epinephrine, norepinephrine, or dopamine were reportedly observed in approximately 20% of patients with neuroblastoma,[1] symptoms due to catecholamine excess are not common in neuroblastoma.[2] Among them, hypertension is relatively common and observed in approximately 10% of patients.[3] Hypertension can occur even in patients with ganglioneuroblastoma[4,5] or ganglioneuroma and is induced by catecholamine excess and for renovascular reasons.[5] Although hypertension is sometimes observed in patents with neuroblastoma,[5–7] the cyclic fluctuation of blood pressure is extremely rare and not reported in the literature. Here we describe a neonatal case of neuroblastoma with cyclic blood pressure fluctuations.

Correspondence: Jun Fujishiro, MD PhD, Department of Pediatric Surgery, Faculty of Medicine, the University of Tokyo, Hongo 7-3-1, Bunkyo-ku, Tokyo 113-8655, Japan. Email: jfujishi-tky@umin.ac.jp

Received 5 March 2014; revised 29 March 2014; accepted 10 April 2014.
doi: 10.1111/ped.12399

J Inherit Metab Dis (2014) 37:801–812
DOI 10.1007/s10545-014-9682-y

ORIGINAL ARTICLE

Clinical, biochemical and molecular analysis of 13 Japanese patients with β-ureidopropionase deficiency demonstrates high prevalence of the c.977G > A (p.R326Q) mutation

Yoko Nakajima · Judith Meijer · Doreen Dobritzsch · Tetsuya Ito · Rutger Meinsma · Nico G. G. M. Abeling · Jeroen Roelofsen · Lida Zoetekouw · Yoriko Watanabe · Kyoko Tashiro · Tomoko Lee · Yasuhiro Takeshima · Hiroshi Mitsubuchi · Akira Yoneyama · Kazuhide Ohta · Kaoru Eto · Kayoko Saito · Tomiko Kuhara · André B. P. van Kuilenburg

Received: 27 August 2013 / Revised: 18 January 2014 / Accepted: 21 January 2014 / Published online: 14 February 2014

Abstract β-ureidopropionase (βUP) deficiency is an autosomal recessive disease characterized by N-carbamyl-β-amino aciduria. To date, only 16 genetically confirmed patients with βUP deficiency have been reported. Here, we report on the clinical, biochemical and molecular findings of 13 Japanese βUP deficient patients. In this group of patients, three novel missense mutations (p.G31S, p.E271K, and p.I286T) and a recently described mutation (p.R326Q) were identified. The p.R326Q mutation was detected in all 13 patients with eight patients being homozygous for this mutation. Screening for the p.R326Q mutation in 110 Japanese individuals showed an allele frequency of 0.9 %. Transient expression of mutant βUP enzymes in HEK293 cells showed that the p.E271K and p.R326Q mutations cause profound decreases in activity

Communicated by:John Christodoulou

Electronic supplementary material The online version of this article (doi:10.1007/s10545-014-9682-y) contains supplementary material, which is available to authorized users.

Y. Nakajima · J. Meijer · R. Meinsma · N. G. G. M. Abeling · J. Roelofsen · L. Zoetekouw · A. B. P. van Kuilenburg
Department of Clinical Chemistry, Laboratory Genetic Metabolic Diseases, Academic Medical Center, 1105 AZ Amsterdam, Netherlands

Y. Nakajima (✉) · T. Ito
Department of Pediatrics and Neonatology, Nagoya City University Graduate School of Medical Sciences, 467-8601 Nagoya, Japan
e-mail: ncu.metabolism@gmail.com

D. Dobritzsch
Department of Chemistry, Uppsala University, BMC, 75123 Uppsala, Sweden

Y. Watanabe
Department of Pediatrics and Child Health, Kurume University School of Medicine, 830-0011 Kurume, Japan

Y. Watanabe · K. Tashiro
Research Institute of Medical Mass Spectrometry, Kurume University School of Medicine, 830-0011 Kurume, Japan

T. Lee · Y. Takeshima
Department of Pediatrics, Kobe University Graduate School of Medicine, 650-0017 Kobe, Japan

H. Mitsubuchi
Department of Neonatology, Kumamoto University Hospital, 860-8556 Kumamoto, Japan

A. Yoneyama
National Rehabilitation Center for Disabled Children, 173-0037 Tokyo, Japan

K. Ohta
Department of Pediatrics, National Hospital Organization Kanazawa Medical Center, 920-8650 Kanazawa, Japan

K. Eto
Department of Pediatrics, Tokyo Women's Medical University, 162-8111 Tokyo, Japan

K. Saito
Institute of Medical Genetics, Tokyo Women's Medical University, 162-0054 Tokyo, Japan

T. Kuhara
Japan Clinical Metabolomics Institute, 929-1174 Kahoku, Japan

(≤ 1.3 %). Conversely, βUP enzymes containing the p.G31S and p.I286T mutations possess residual activities of 50 and 70 %, respectively, suggesting we cannot exclude the presence of additional mutations in the non-coding region of the *UPB1* gene. Analysis of a human βUP homology model revealed that the effects of the mutations (p.G31S, p.E271K, and p.R326Q) on enzyme activity are most likely linked to improper oligomer assembly. Highly variable phenotypes ranging from neurological involvement (including convulsions and autism) to asymptomatic, were observed in diagnosed patients. High prevalence of p.R326Q in the normal Japanese population indicates that βUP deficiency is not as rare as generally considered and screening for βUP deficiency should be included in diagnosis of patients with unexplained neurological abnormalities.

Introduction

Pyrimidine nucleotides play an important role in various biological processes, including synthesis of RNA, DNA, phospholipids, uridine diphosphate glucose and glycogen. Intracellular pools of pyrimidines are produced de novo through salvage and catabolic pathways (Huang and Graves 2003; Traut 1994), and in humans, the pyrimidine bases uracil and thymine, are degraded via three enzymatic steps (Wasternack 1980). Dihydropyrimidine dehydrogenase (DPD, EC 1.3.1.2) is the initial and rate-limiting enzyme, catalyzing uracil and thymine reduction to 5,6-dihydrouracil and 5,6-dihydrothymine, respectively. The second enzyme, dihydropyrimidinase (DHP, EC 3.5.2.2), catalyzes the hydrolytic ring opening of the dihydropyrimidines. The third step, catalyzed by β-ureidopropionase (βUP) (EC 3.5.1.6), results in conversion of N-carbamyl-β-alanine and N-carbamyl-β-aminoisobutyric acid into β-alanine and β-aminoisobutyric acid, respectively, with concomitant production of ammonia and carbon dioxide.

Higher eukaryotic βUP belong to the nitrilase superfamily of enzymes (Pace and Brenner 2001). The closest known structural relative of human βUP is found in *Drosophila melanogaster* (DmβUP) (Lundgren et al 2008), sharing 63 % amino acid sequence identity. In solution, DmβUP exists as a mixture of oligomers but crystallizes as a homooctamer. It has a helical-turn like structure that is consecutively built up from dimeric units. This is in contrast to other members of the nitrilase superfamily that assemble their homotetrameric or homohexameric native states in a markedly different fashion, and is most likely because of an N-terminal ~65 amino acid extension unique to βUPs.

βUP deficiency (MIM 606673) is an autosomal recessive disease caused by mutations in the βUP gene, *UPB1*. The *UPB1* gene maps to chromosome 22q11.2, and consists of ten exons spanning approximately 20 kb of genomic DNA (Vreken et al 1999). To date, only 16 genetically confirmed patients with βUP deficiency have been reported (van Kuilenburg et al 2012). The clinical phenotype of these patients is highly variable, but tends to center around neurological problems (van Kuilenburg et al 2012). However, in Japan, four asymptomatic individuals have been detected through newborn screening by gas chromatography-mass spectrometry (GC/MS), and the prevalence of βUP deficiency in Japan has been estimated to be one in 6000 (Kuhara et al 2009). Thus, the clinical presentation and biochemical and genetic spectrum of patients with βUP deficiency are still largely unknown.

In this study, we report genetic and biochemical analysis, and clinical follow-up findings, of 13 Japanese patients (including seven newly identified individuals) with βUP deficiency. Functional and structural consequences of the mutations at the protein level were analysed using a eukaryotic expression system and a homology model generated based on the crystal structure of recombinant DmβUP.

Materials and methods

Patients

Patients 1, 2 and 3, who presented with neurological abnormalities during early childhood were detected through a high-risk urine screening for general metabolic disorders performed at Kanazawa Medical University (Ohse et al 2002). In general patients are tested for metabolic disorders if patients presented with developmental delay, hyperammonemia, metabolic acidosis and neurological manifestations such as convulsions, autism and related disorders. Patients 4–7 and 8–13 were from two different areas in Japan, detected in a pilot study screening for inborn errors of metabolism by GC/MS in newborn urine samples, and conducted at Kanazawa Medical University (Kuhara et al 2009) (patients 4–7) and Kurume University (patients 8–13). After informed consent was obtained from their parents, urine and blood samples from all patients were sent to the Laboratory for Genetic Metabolic Diseases in Amsterdam, the Netherlands for further analysis.

Quantitative pyrimidine analysis

On the basis of a gross elevation of N-carbamyl-ß-alanine and N-carbamyl-ß-aminoisobutyric acid in urine screening for inborn errors of metabolism by GCMS (Ohse et al 2002), ß-ureidopropionase deficiency was suspected. Subsequently, quantitation of relevant pyrimidines and its metabolites was performed by HPLC tandem mass spectrometry. Concentrations of uracil, thymine, dihydrouracil,

dihydrothymine, N-carbamyl-β-alanine and N-carbamyl-β-aminoisobutyric acid, in urine-soaked filter paper strips, were determined using reversed-phase HPLC-tandem mass spectrometry (HPLC-MS/MS) (van Kuilenburg et al 2004c; van Lenthe et al 2000).

PCR amplification of *UPB1* coding exons

DNA was isolated from whole blood or blood spots using the QIAamp DNA Micro kit (QIAGEN). Exons 1-10 and flanking intronic regions of *UPB1*, were amplified using previously described primer sets (van Kuilenburg et al 2004a). *UPB1* sequence from patients was compared to controls and the reference *UPB1* sequence (Ref Seq NM_016327.2).

Cloning and site-directed mutagenesis

An expression plasmid containing wild-type human βUP cDNA (pSE420-βUP) was constructed by subcloning the complete coding region of human *UPB1* into the *Nco*I-*Nae*I site of the pSE420 vector (Vreken et al 1999). The *UPB1* coding sequence was then re-cloned into the *BamH*I-*Kpn*I site of the pcDNA3.1Zeo vector, which includes coding sequence for a cleavable C-terminal 6-His-fusion tag. To introduce mutations, the pcDNA3.1Zeo plasmid containing wild-type *UPB1* was subjected to site-directed mutagenesis. Compatible primers (Table 1S, Supplementary data) were designed for use with the QuikChange™ Site-Directed Mutagenesis Kit (Life technologies). PCR-mediated site-directed mutagenesis was performed according to the manufacturer's recommended protocol. All resulting plasmids were sequenced to confirm introduction of single nucleotide changes.

Cell culture and transient transfection

HEK293 cells were cultured in Dulbecco's modified eagle's medium with 4.5 g/L glucose, 25 mM Hepes and 584 mg/L L-glutamine (Lonza), supplemented with 10 % fetal bovine serum, 100 U/ml penicillin, 100 mg/ml streptomycin and 250 μg/ml fungizone at 37 °C in a humidified 5 % CO_2 incubator. For transient transfections, cell cultures were set up in six-well plates 24 h prior to transfection. HEK293 cells were transfected with pcDNA3.1Zeo-βUP (wild-type or variants) using X-treme GENE HP DNA Transfection reagent (Roche). Two days after transfection, cells were harvested and washed with PBS. After centrifugation at 1000×g for 5 min at 4 °C, cell pellets were immediately frozen in liquid nitrogen and stored at−80 °C until use. All transfections were performed in at least triplicate. Parental vector (pcDNA3.1Zeo) without insert was transfected as negative control.

βUP enzyme activity assay

Cell pellets were resuspended in 300 μl isolation buffer (35 mM potassium phosphate, pH 7.4 and 2.5 mM $MgCl_2$) and lysed by sonication on ice. Crude lysates were centrifuged at ≥ 11,000 rpm for 20 min at 4 °C, and then supernatant protein concentrations and βUP enzyme activity of the expressed protein directly quantified. βUP activity was determined at 37 °C in a standard assay mixture containing cell supernatant, 200 mM Mops (pH 7.4), 1 mM dithiothreitol and 500 μM [^{14}C]-N-carbamyl-β-alanine, as described previously (Van Kuilenburg et al 1999).

Western blot analysis

Cell supernatants containing 5 μg protein were fractionated on NuPAGE® 4–12 % Bis-Tris Mini Gels (Life technologies) and transferred to nitrocellulose membranes. Membranes were blocked using Odyssey blocking buffer (LI-COR). Subsequently, blots were incubated for one hour with a 1:1000 dilution of rabbit anti-UPB1 (Anti-UPB1 AV42467-100UG, Sigma-Aldrich) and 1:5000 dilution of mouse anti-alpha-tubulin antibodies in blocking buffer (50 % Odyssey blocking buffer, 50 % PBS and 0.1 % Tween). Membranes were washed three times and then incubated for one hour with a 1:10,000 dilution of IRDye800 conjugated goat anti-rabbit and IRDye680 conjugated donkey anti-mouse (both LI-COR) secondary antibodies, in the same blocking buffer as used for primary antibodies, with 0.01 % SDS. Blots were scanned and band intensities analysed using the LI-COR Odyssey infrared imaging system.

Native gel electrophoresis

Blue native polyacrylamide gel electrophoresis was performed using 4–16 % NativePAGE™ Novex® Bis-Tris Gels (Life technologies). Supernatant samples were prepared in sample buffer (50 mM Bis Tris, 6 N HCL, 50 mM NaCl, 10 % glycerol and 0.001 % Ponceau S, pH 7.2), and 5 μg protein loaded. Electrophoresis was performed at 100 V for 2 h at room temperature. Gels were transferred onto PVDF membranes and immunoblotting performed, as described above. NativeMark™ Unstained Protein Standard (Life technologies) was used as a molecular weight marker, and visualized with Ponceau S staining after western transfer.

Crystal structure analysis

A homology model of human βUP was generated using the SWISSMODEL server, based on the crystal structure of *Drosophila melanogaster* βUP (DmβUP) (PDB-ID:2vhi

and 2vhh) (Lundgren et al 2008). WinCoot (Emsley et al 2010) was used for structural analysis and manual introduction of amino acid exchanges resulting from *UPB1* mutations. Energetically preferred side chain conformations causing the least steric clashes and optimal interactions with surrounding residues were chosen. Figure 1 was generated using PyMol (DeLano 2002).

Genotyping of c.977G > A by PCR-based restriction fragment length polymorphism (PCR-RFLP) analysis

A 333 bp fragment of genomic DNA was amplified using a primer set used for mutation analysis of exon 9 of the *UPB1* gene. The amplified product was digested using the restriction enzyme *Msp*I, for 2 h at 37 °C. Transition of G to A at c.977

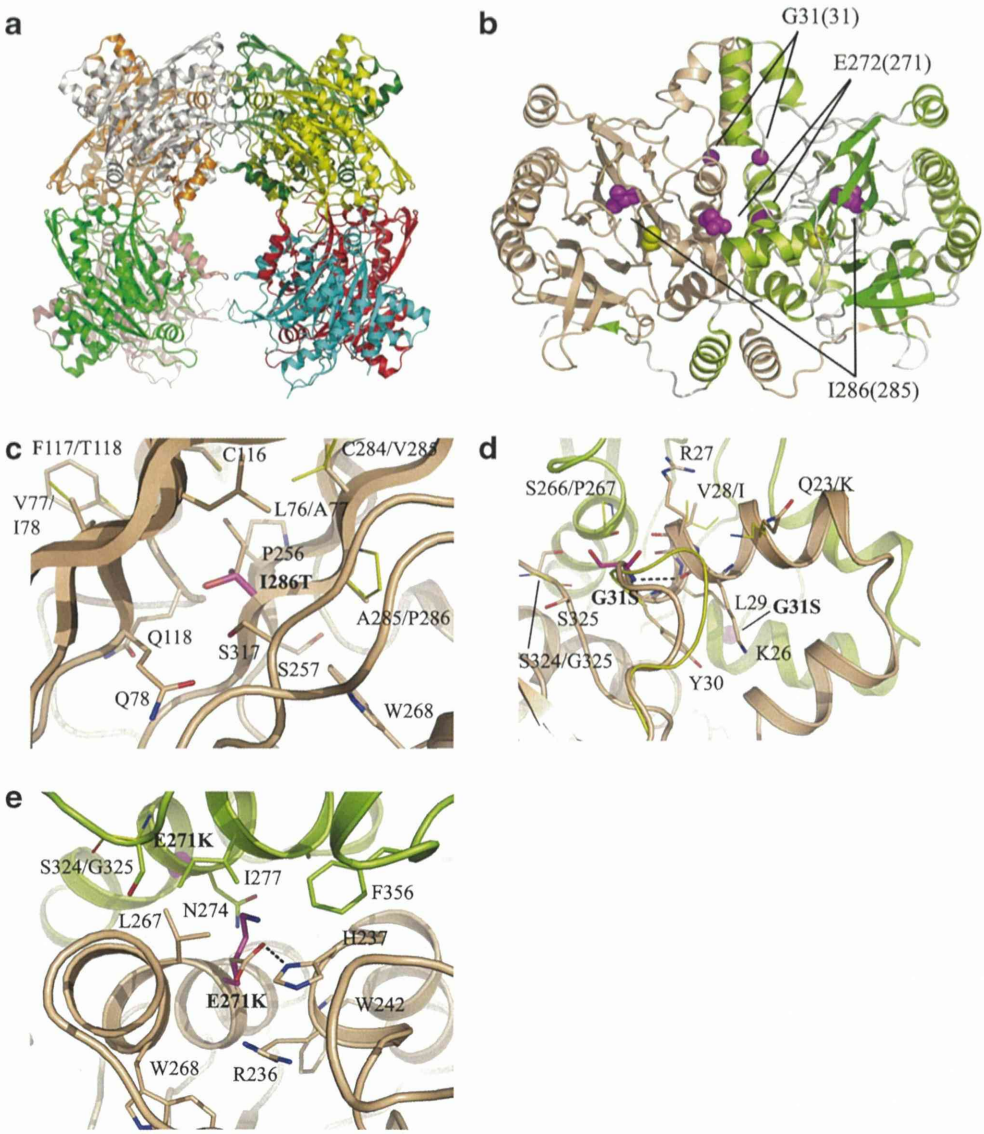

Fig. 1 DmβUP crystal structure and mutation site environment in the homology model of human βUP. (**a**) Schematic view of homooctameric DmβUP with each subunit coloured differently. (**b**) Schematic view of a dimeric unit of DmβUP. For one of the subunits, β-strands are depicted in green, helices in yellow-green and loops in white, with the other subunit coloured salmon. Mutation sites are highlighted by space-filling models of the respective amino acid side chains in magenta. Labels first list the corresponding site in DmβUP. Location of the active site is indicated by space-filling models of the active site cysteine (C233 in human βUP, C234 in DmβUP) in yellow. (**c-e**) Enlarged views of I286T, G31S and E271K mutation sites. The homology model of human βUP is shown with different colours (salmon and green) for two separate subunits. Additional subunits were omitted as none of the mutations occur near putative interfaces. Stick models of side chains introduced by the mutations are shown in magenta, in preferred conformations causing the least clashes. Native side chains and residues surrounding the site are depicted with carbon atoms in the same colour as the subunit to which they belong. DmβUP side chains are shown with yellow carbon atoms when not conserved in human βUP. Labels indicate human βUP residues followed by corresponding DmβUP residues (if shown), with numbering for the latter only when it differs. Hydrogen bonds are indicated by dotted black lines. In (d), the loop directly following the G31S site is extended by one amino acid in DmβUP (shown in yellow). In (d) and (e), corresponding mutation sites in the second subunit of the dimer are marked by a magenta sphere in the background

abolishes a restriction site in the mutant allele. Digested products were separated on 2.8 % agarose gels stained with ethidium bromide. Genotypes were identified as wild-type (GG) (three bands of 192, 153 and 24 bp), heterozygous mutant (GA) (bands of 216, 192, 153 and 24 bp), or homozygous mutant (AA) (bands of 216 and 153 bp).

In addition, the frequency of the c.977G > A mutation was assessed in the exome variant server (EVS) of the National Heart, Lung, and Blood Institute GO Exome Sequencing Project (Seattle, WA, USA; URL: evs.gs.washington.edu/EVS/) with the corresponding nucleotide positions being analysed in >8.000 European and >4.000 African American alleles, and in the Database of Single Nucleotide Polymorphisms (dbSNP; Bethesda: National Center for Biotechnology Information, National Library of Medicine [dbSNP Build ID: 137]; available from: http://www.ncbi.nlm.nih.gov/SNP/).

Results

Clinical evaluation

All patients were born to healthy non-consanguineous Japanese parents. Patient 1 was a girl born at full term following an uneventful delivery. At the age of two months, she was irritable and had occasional jerky eye movements, with impairment of visual contact noticed. A week later she presented with infantile spasms, and head-nodding three to four times a day. Cortical dysplasia was suspected from head MRI, and EEGs showed hypsarrhythmia. She was diagnosed with West syndrome. Biochemical investigation of urine obtained during her first admission revealed significantly increased levels of N-carbamyl-β-alanine and N-carbamyl-β-aminoisobutyric acid (Kuhara et al 2009). The infantile spasms and abnormal EEGs did not respond to zonisamide, therefore adrenocorticotropic hormone (ACTH) therapy was started at three months of age, and subsequently, the seizures disappeared and EEG abnormalities subsided. At the age of 5 years, she had partial seizures occasionally but her development was within the normal range.

Patient 2 was a 3-year old boy who presented with autism and mild mental retardation. At the age of 18 months, his parents noticed social communication impairments, including eye-to-eye gazing, facial expression, and language understanding. At the age of 3.5 years, he was diagnosed with autism. When he was 8 years old, he developed a sleep disorder and melatonin treatment was started. The Wechsler Intelligence Score for Children test, performed at 11 years of age, revealed a full scale IQ of 71, verbal IQ of 66, and performance IQ of 83. He now attends a special-needs school.

Patient 3 was a 12-month old boy who presented with mild hypotonia and motor developmental delay. The family history found a 15-year old male cousin from the paternal side suffers from epilepsy and autism related disorder. At the follow-up age of 2.8 years, his motor development caught up to the normal range but he has developed mild mental retardation, particularly in speech development.

Patients 4–7 were detected through neonatal screening performed from 1996 to 2009 in Kanazawa (Kuhara et al 2009). Since screening, they have been followed regularly by an attending paediatrician. Patient 4 is a boy who developed neurological symptoms during the follow-up period. At the age of 12 months, he had an attack of sudden-onset consciousness impairment, a blank stare, and unresponsiveness which lasted for 2–3 min. A year after this episode, he developed febrile seizures that occurred four times. One of the attacks lasted over 30 min and was not easily controlled. The laboratory investigation at admission showed no abnormalities. His fever abated the following day and he regained consciousness. Further investigations by head MRI and EEG were normal. He has had no seizures since 3 years of age, owing to the use of diazepam suppositories during fevers. At 5 years of age, he has normal growth and development.

Patients 5 and 6 are twin sisters, born at 36 weeks gestation with birth weights of 2042 g and 2378 g, respectively. During a follow-up period of 5 years, patient 6 showed no physical examination abnormalities. Patient 5 has a height within the 3–10 percentile range and has developed hypermetropia. Patient 7 is a 10-year-old boy with an unremarkable history and no clinical manifestations during follow-up. Patients 8–13 were detected from newborn screening performed in Kurume during a period from February 2010 to January 2012. None of them showed abnormal developmental milestones at follow-up evaluation.

Pyrimidine bases and degradation metabolites in urine

Urinary quantitative analysis of relevant pyrimidines and metabolites was performed by HPLC-MS/MS. Urinary concentrations of the 13 patients are shown as subdivided genotype groups (Fig. 2). All urine samples from the patients showed strongly elevated levels of N-carbamyl-β-alanine and N-carbamyl-β-aminoisobutyric acid, and moderately elevated levels of dihydrouracil and dihydrothymine. Mean concentrations of uracil (25.5±11.4 μmol/mmol creatinine), thymine (3.6±1.9 μmol/mmol creatinine), dihydrouracil (57±27 μmol/mmol creatinine), and dihydrothymine (127±65 μmol/mmol creatinine), were 2-, 7-, 9-, and 41–fold, respectively, higher compared with mean concentrations observed in controls. Additionally, mean concentrations of N-carbamyl-β-alanine (648±208 μmol/mmol creatinine) and N-carbamyl-β-aminoisobutyric acid (504±297 μmol/mmol creatinine) were 59-and 276-fold, respectively, higher compared to mean concentrations observed in controls. The observed N-

carbamyl-β-amino aciduria in these patients strongly suggests βUP deficiency.

Mutation analysis of *UPB1*

Sequencing exons 1–10 (including flanking intronic regions) of *UPB1* in the 13 patients, identified one previously described missense (c.977G>A) and three novel missense (c.91G>A, c.811G>A, and c.857 T>C) mutations (Table 1). This table also includes 15 patients (from 12 families) with βUP deficiency, and previously published mutations (Assmann et al 1998; Assmann et al 2006; van Kuilenburg et al 2012; Yaplito-Lee et al 2008). All 13 Japanese patients were carriers of the c.977G>A (p.R326Q) mutation, with eight patients being homozygous for this mutation (Table 1). Distribution of the *UPB1* mutations within the exons is shown (Fig. 3a). All previously identified mutations and the three novel missense mutations were located in exons 1, 2, and 6–10.

Functional analysis and expression of mutant βUP protein

Recombinant wild-type and four βUP proteins containing the mutations, p.G31S, p.E271K, p.I286T, and p.R326Q, were expressed in HEK293 cells. No endogenous βUP activity (< 0.7 nmol/mg/h) was detected in HEK293 cells. Activity of wild-type βUP protein was 1976±416 nmol/mg/h (n=9). Recombinant βUP enzymes carrying mutations p.E271K and p.R326Q, exhibited 0.7 and 1.3 %, respectively, of wild-type activity, whereas βUP enzymes containing mutations p.G31S and p.I286T, possessed residual activities of 51.6 and 69.8 %, respectively (Fig. 3b).

Immunoblot analysis of expression levels of βUP mutant proteins in soluble extracts from transfected HEK293 cells, showed mutant proteins were expressed in comparable amounts as wild-type protein (Fig. 3c).

Western blotting of blue native gels detected various high molecular weight oligomeric forms of wild-type βUP, comparable or identical to that observed for βUP enzymes containing p.G31S and p.I286T mutations. In contrast, no distinct sharp bands of high molecular weight were observed for βUP enzymes containing p.E271K and p.R326Q mutations, although bands of lower molecular weights were present, corresponding to lower oligomeric states (from monomers to octamers) of βUP (Fig. 3d). These lower molecular weight species were also observed in extracts from wild-type, p.G31S and p.I286T expressing cells, albeit with evidently lower intensity. This indicates that p.E271K and p.R326Q proteins have a dramatically reduced ability to form larger oligomers, and thus, their potential equilibrium of oligomerization status was shifted towards lower molecular weight species.

Fig. 2 Pyrimidine and metabolite concentrations in urine of βUP deficient patients and controls. Patients are classified in terms of their genotype. (**a**) N-carbamyl-β-alanine, (**b**) N-carbamyl-β-aminoisobutyric acid, (**c**) dihydrouracil, (**d**) dihydrothymine, (**e**) uracil, and (**f**) thymine. In controls, the top, bottom and line through the middle of a box, correspond to the 75th, 25th and 50th percentiles, respectively. Whiskers on the bottom extend from the 2.5th percentile, and on the top, the 97.5th percentile

Population study of βUP deficiency and the p.R326Q mutation

Three patients with βUP deficiency were identified out of 4500 patients of a high-risk screening group demonstrating that the prevalence of βUP deficiency in a high-risk screening group is one in 1500. PCR-RFLP analysis of the c.977G>A (p.R326Q) mutation was performed in 110 Japanese healthy controls. We identified two individuals heterozygous for the p.R326Q mutation, and no homozygous individuals, resulting in a frequency of heterozygotes in the Japanese population of 1.8 % (an allele frequency of 0.91 %). Analysis of publically available databases showed that the c.977G>A mutation was not detected in >8.000 European and >4.000 African American alleles whereas the mutation was detected with an allele frequency of 2.6 % in 286 individuals of East Asian ancestry.

Analysis of the structural effects of *UPB1* mutations by homology modelling

A homology model of human βUP was generated to predict the effect of the *UPB1* mutations on enzyme structure. High sequence similarity between homologous enzymes at mutation sites (with G31 and E271 being strictly conserved in deposited βUP sequences, and I286 replaced by leucine in rodent enzymes only) suggests the mutations occur within structurally conserved regions.

I286 is located in the subunit core, approximately at 10 Å distance from the active site (Fig. 1b). It is surrounded by hydrophobic and polar residues (Fig. 1c). The increase in side chain polarity upon mutation to threonine may therefore be tolerated, and structural adjustments limited to orientation of the hydroxyl group towards polar neighbours and re-optimization of side chain packing, with minor effects on active site geometry and enzymatic activity. This correlates well with the measured residual activity, and unaltered behaviour of the mutant protein in native gel analysis.

G31 is located directly downstream of a helix involved in dimer interface formation in DmβUP (Fig. 1d) (Lundgren et al 2008). Mutation to serine requires structural rearrangement as the close proximity of S325 leaves little space for a side chain.

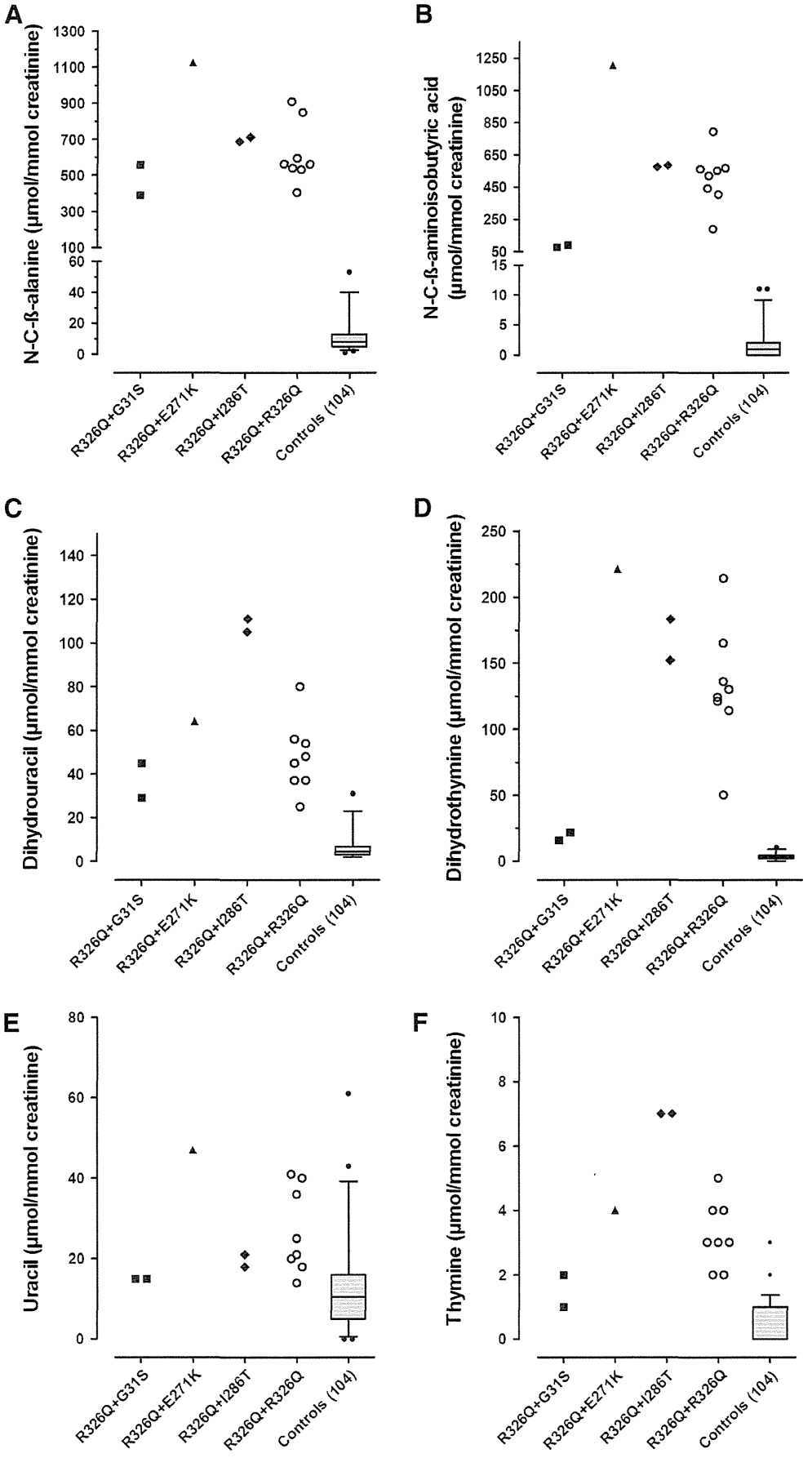
A
N-C-ß-alanine (µmol/mmol creatinine)
1300
1100
900
700
500
300
100
60
40
20
0
R326Q+G31S
R326Q+E271K
R326Q+I286T
R326Q+R326Q
Controls (104)
B
N-C-ß-aminoisobutyric acid (µmol/mmol creatinine)
1250
1050
850
650
450
250
50
15
10
5
0
C
Dihydrouracil (µmol/mmol creatinine)
140
120
100
80
60
40
20
0
D
Dihydrothymine (µmol/mmol creatinine)
250
200
150
100
50
0
E
Uracil (µmol/mmol creatinine)
80
60
40
20
0
F
Thymine (µmol/mmol creatinine)
10
8
6
4
2
0

Table 1 Genetic and phenotypic findings of patients with β-ureidopropionase deficiency

Patient No.	Origin	Consanguinity	Sex	Age at diagnosis (years)	Age at follow-up (years)	Symptom	Genotype	Effect	Location	Reference
1	Japan	-	F	0.2	5.0	Seizures (West syndrome)	c.[977G > A] + [977G > A]	p.[R326Q] + [R326Q]	Ex 9	van Kuilenburg, et al 2012
2	Japan	-	M	3.5	16.0	MR, Autism	c.[977G > A] + [977G > A]	p.[R326Q]+[R326Q]	Ex 9	Present study
3	Japan	-	M	1.0	2.8	Motor retardation MR	c.[811G > A] + [977G > A]	p.[E271K]+[R326Q]	Ex 7, Ex 9	Present study
	Turkey[a)]	+	M	0.8	NA	Seizures	c.[1076C > T] + [1076C > T]	p.[T359M]+[T359M]	Ex 10	van Kuilenburg, et al 2012
	Egypt[b)]	+	F	Birth	NA	Seizures, MC	c.[105-2A > G] + [105-2A > G]	splicing	Int 1	van Kuilenburg, et al 2012
	Egypt[b)]	+	M	Birth	NA	Seizures, MC	No DNA available			van Kuilenburg, et al 2012
	Egypt	+	M	0.8	NA	Seizures, MR, hypotonia	c.[38 T> C] + [38 T > C]	p.[L31S]+[L31S]	Ex 1	van Kuilenburg, et al 2012
	Pakistan	+	F	2.0	NA	MC, MR, hypotonia, Autism	c.[792C > A] + [873 + 1G > A]	p.[S264R]+splicing	Ex7, Int 7	van Kuilenburg, et al 2012
	China	−	M	1.1	NA	MC, MR	c.[977G > A] + [977G > A]	p.[R326Q] + [R326Q]	Ex 9	van Kuilenburg, et al 2012
	Germany	−	F	0.9	NA	Seizures, hypotonia	c.[703 > A] + [917-1G > A]	p.[G235R] + splicing	Ex 6, Int 8	van Kuilenburg, et al 2012
	China	−	M	3.0	NA	MR	c.[706C > T] + [792C> A]	p.[R236W] + [S264R]	Ex 6, Ex 7	van Kuilenburg, et al 2012
	Turkey	+	F	5.3	NA	MR, hypotonia	c.[105-2A > G] + [917-1G > A]	splicing	Int 1, Int 8	Assmann et al 1998; van Kuilenburg 2004
	Turkey	+	F	3.0	NA	Seizures, MR	c.[105-2A > G] + [105-2A > G]	splicing	Int 1	van Kuilenburg 2004
	Germany	−	M	0.9	NA	Seizures, MC, MR, hypotonia	c.[917-1G > A] + [917-1G > A]	splicing	Int 8	Assmann et al 2006; van Kuilenburg 2004
	African	−	F	1.0	NA	Seizures	c.[254C > A] + [254C > A]	p.[A85E] + [A85E]	Ex 2	van Kuilenburg 2004
	Australia	−	M	1.0	NA	Urogenital and colorectal system anomalies	c.[209G > C] + [105-2A > G]	p.[R70P] + splicing	Ex 2 Int 1	Yaplito-Lee et al 2008
	Turkey[a)]		F	30, CT	NA	AS	c.[1076C > T] + [1076C > T]	p.[T359M] + [T359M]	Ex 10	van Kuilenburg, et al 2012
	Egypt[b)]		M	27, CT	NA	AS	c.[105-2A > G] + [105-2A > G]	splicing	Int 1	van Kuilenburg, et al 2012
4	Japan	−	M	NS	5.3	Absence seizure, febrile seizure	c.[977G > A] + [977G > A]	p.[R326Q] + [R326Q]	Ex 9	Present study
5*	Japan	−	F	NS	5.5	AS	c.[857 T > C] + [977G > A]	p.[I286T] + [R326Q]	Ex7, Ex9	Present study
6*	Japan	−	F	NS	5.5	AS, hypermetropia	c.[857 T > C] + [977G > A]	p.[I286T] + [R326Q]	Ex7, Ex9	Present study
7	Japan	−	M	NS	10.5	AS	c.[977G > A] + [977G > A]	p.[R326Q] + [R326Q]	Ex 9	Present study
8	Japan	−	M	NS	2.5	AS	c.[977G > A] + [977G > A]	p.[R326Q] + [R326Q]	Ex 9	Present study
9	Japan	−	F	NS	2.9	AS	c.[977G > A] + [977G > A]	p.[R326Q] + [R326Q]	Ex 9	Present study
10	Japan	−	M	NS	1.3	AS	c.[91G > A] + [977G > A]	p.[G31S] + [R326Q]	Ex1, Ex 9	Present study
11	Japan	−	F	NS	2.3	AS	c.[977G > A] + [977G > A]	p.[R326Q] + [R326Q]	Ex 9	Present study
12	Japan	−	F	NS	1.7	AS	c.[977G > A] + [977G> A]	p.[R326Q] + [R326Q]	Ex 9	Present study
13	Japan	−	F	NS	1.1	AS	c.[91G > A] + [977G > A]	p.[G31S] + [R326Q]	Ex1, Ex 9	Present study

NA = not available, NS = neonatal screening, CT = carrier testing, AS = asymptomatic, MR = mental retardation, MC = microcephaly,

* Patient 5 and 6 are twin siblings. [a)] indicates same family members (child and mother). [b)] indicates same family members (two siblings and father)

Biochemical data of patient 1, 2, 4, 5, 6 and 7 were previously reported (Kuhara et al 2009)

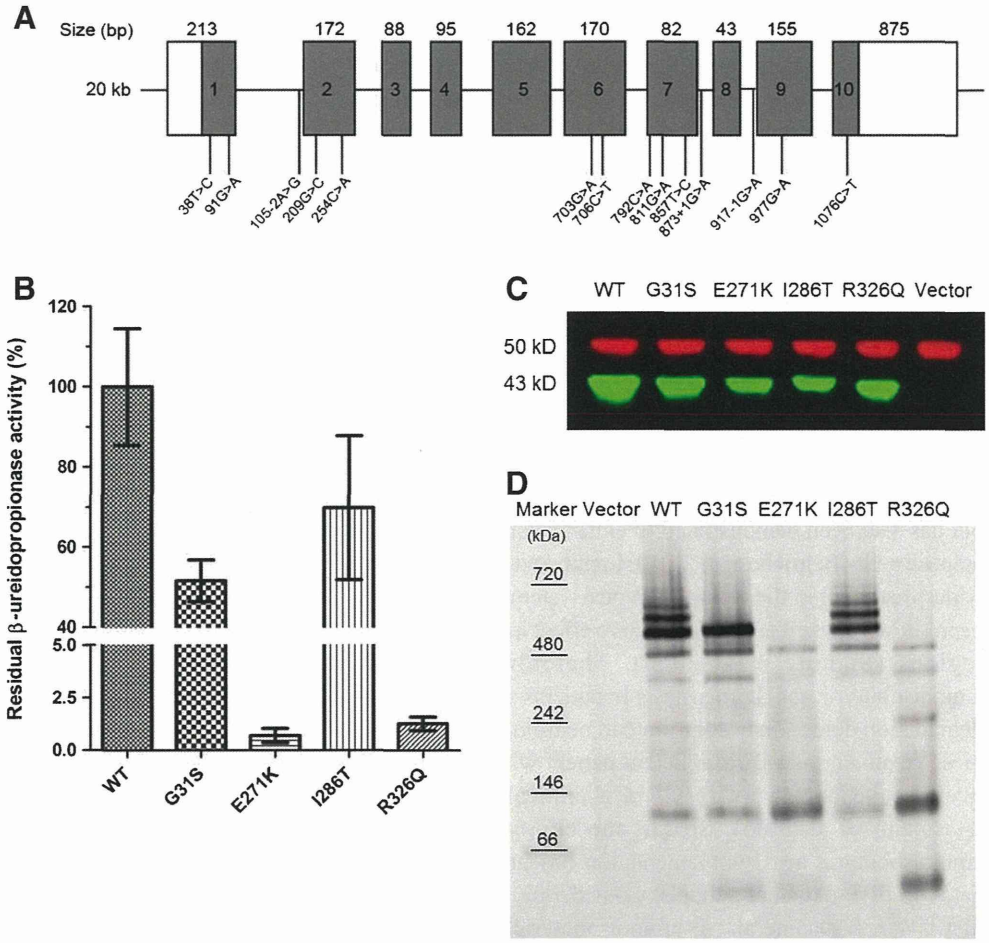

Fig. 3 (**a**) Schematic representation of genomic organization of the *UPB1* gene. *UPB1* consists of ten exons encoding an open reading frame of 1152 bp (depicted in grey). The mutations identified to date in βUP deficient patients are indicated, with numbers corresponding to cDNA positions. (**b**) Expression of βUP mutants in HEK293 cells. Residual enzymatic activity of βUP mutants are expressed as percentages of wild-type βUP activity. For each construct, columns show mean values and standard deviations derived from at least three transfections. (**c**) Western blot analysis of HEK293 cells expressing wild-type and mutant βUP. Total cell protein (5 μg) was resolved by SDS-PAGE followed by immunoblotting against βUP and alpha-tubulin. (**d**) Native polyacrylamide gel electrophoresis of HEK293 cells expressing βUP protein (wild-type and mutants). Cell supernatants (5 μg) were subjected to 4–16 % blue native page, followed by western blot analysis using polyclonal anti-βUP antibody

Taking into account that several previously identified deleterious mutations also cluster at oligomerization surfaces (van Kuilenburg et al 2012), the significant loss in enzyme activity is most likely linked to disturbance of subunit interactions. Interestingly, native gel electrophoresis showed that only formation of larger assemblies (those exceeding the size of octamers) is hampered.

In DmβUP, the glutamate corresponding to E271 interacts with two basic residues that are both conserved in the human enzyme (H237, R236) (Fig. 1e). For the E271K mutant, clashes of lysine 271 with nearby residues, and placement of its positively charged head group in a hydrophobic (L267, I277 and F356) or similarly charged environment (H237 and R236), will have severely destabilizing effects, further amplified by the proximity of corresponding mutation sites of two subunits at the dimer interface (Fig. 1e). Structural changes to accommodate the altered side chain are likely to affect oligomerization, as confirmed by native gel electrophoresis (Fig. 3d). As the helix carrying E271 is placed beside the one harbouring C233, any shifts in its position may also directly influence active site geometry and cause the observed dramatic loss of enzymatic activity.

Discussion

βUP deficiency is described as exhibiting variable phenotypic presentation, ranging from early infantile onset with severe neurological involvement, to mild developmental delay and learning disabilities, to asymptomatic individuals (van Kuilenburg et al 2012). Despite large variation in clinical presentation, the majority of previously identified patients (85 %) present with MRI abnormalities (van Kuilenburg et al 2012). In the present study, only three of the 13 patients had neurological problems during infancy, and underwent biochemical urine analysis as part of diagnostic examinations. Ten of the patients were identified through newborn screening programs. Follow-up clinical investigation revealed that one of these patients had suffered from an episode of unconsciousness, and later developed febrile seizures. To date, the nine other individuals have remained asymptomatic. As the follow-up period of some patients (specifically, patients 8–13) is relatively short, being only one to two years, it is conceivable that more patients may present with a clinical phenotype in due course.

The clinical phenotype of patients with DHP and DPD deficiencies, the other two biochemical defects occurring

within the pyrimidine degradation pathway, is highly variable, ranging from severely (neurologically) affected to symptomless. The underlying pathogenesis of these variable clinical manifestations of pyrimidine degradation disorders remains, as yet, unknown. However, similarities between clinical phenotypes of patients with βUP deficiency, and DHP and DPD deficiencies, suggests loss of physiological function of the absent pathway metabolites, rather than toxicity of the accumulated metabolite, is the underlying cause. In this respect, patients with pyrimidine degradation defects show normal to slightly decreased β-alanine levels in plasma and normal levels in CSF, whereas β-aminoisobutyric acid concentrations are strongly reduced in plasma and CSF (van Kuilenburg et al 2004a, b, 2008). β-Aminoisobutyric acid is not only a partial agonist of the glycine receptor (Schmieden and Betz 1995), but has also been demonstrated to enhance leptin secretion in adipose cells (Begriche et al 2010). Leptin and its receptors are widespread within the central nervous system, and leptin has been shown to exert a neuroprotective effect in damaged brain regions (Signore et al 2008). Therefore, altered β-aminoisobutyric acid homeostasis in patients with pyrimidine degradation defects may contribute to neurological abnormalities. Treatment of a ßUP-deficient patient with ß-alanine for over 1.5 years did not result in a clinical improvement (Assmann et al 2006). So far, the clinical effect of ß-aminoisobutyric acid supplementation has not been investigated in ßUP-deficient patients. Considering the pivotal role of βUP in β-alanine and β-aminoisobutyric acid synthesis, we suspect it is unlikely that βUP deficiency is not related at all to the neurological presentation observed in some of our patients. However, our observation that patients with βUP deficiency can present without any clinical abnormalities suggests additional factors are involved in the clinical outcome. These additional factors likely include alterations in other genes and/or environmental factors.

Until now, eight missense and three splice site mutations in *UPB1* have been identified in patients with βUP deficiency (van Kuilenburg et al 2012). In this study, we identified three novel missense mutations and one recently reported mutation, p.R326Q, in 13 patients from 12 unrelated Japanese families. It is noteworthy that homozygosity of the p.R326Q mutation is observed in 62 % (8/13) of Japanese patients, and all 13 patients carried this mutation on one or both alleles, resulting in an allele frequency of 81 % (21/26) in Japanese patients with βUP deficiency. Based on the fact that 1.8 % of the Japanese population is heterozygous for the p.R326Q mutation, we estimate that one individual per 12,500 will be homozygous for the p.R326Q mutation. Thus, compared with other frequently occurring inborn errors of metabolism, such as phenylketonuria (1:70,000 in Japan), the expected prevalence of βUP deficiency is not as rare as generally considered.

The fact that none of the patients identified through newborn screening had lasting neurological problems, in combination with the high estimated prevalence in Japan and variable features in diagnosed patients, may indicate that the disease has low penetrance and is a risk factor. However, it may be too early to conclude that penetrance is low as we cannot exclude the possibility that these patients will develop symptoms later on in life. In addition, the prevalence of ß-ureidopropionase deficiency in a high-risk group is four-times higher (1:1500) than that observed in a control population (1:6000) (Kuhara et al 2009). This observation suggests that ß-ureidopropionase deficiency might be involved in the onset of a clinical phenotype.

Expression of mutant βUPs showed that p.E271K and p.R326Q mutants exhibit significantly decreased residual activity, whereas p.G31S and p.I286T mutants have more than 50 % residual activity of wild type. This result is to some extent in agreement with the finding that the two patients heterozygous for p.G31S present with relatively low urinary N-carbamyl-β-aminoisobutyric acid concentrations, although this was not apparent in two siblings heterozygous for p.I286T (Fig. 2). In combination with the blue native gel analysis, there is no convincing evidence that the p.G31S or p.I286T mutations are pathogenic. Since no DNA of the parents was available, carriership analysis of the mutations could not be performed. Therefore, it is conceivable that c.91G > A (p.G31S) and c.857 T > C (p.I286T) are in *cis* with c.977G > A (p.R326Q). Thus, we cannot exclude the possibility that additional mutations may be present within non-coding regions of *UPB1* in patients carrying p.G31S or p.I286T mutations.

Recently, heterologous expression of p.R326Q mutant βUP in *E.coli* was shown to result in mutant enzyme with no residual activity (van Kuilenburg et al 2012). Similarly, in the present study, expression of p.R326Q mutant enzyme in HEK293 cells caused a dramatic decrease in residual activity. The wide-ranging urinary levels of N-carbamyl-β-alanine and N-carbamyl-β-aminoisobutyric acid observed in patients homozygous for the p.R326Q mutation (Fig. 2), suggest there is no clear correlation between urinary biochemical phenotype and genotype in this group of patients. In addition, identification of the p.R326Q mutation in both neurologically affected patients and unaffected individuals indicates the severity of βUP deficiency is not determined exclusively by *UPB1* mutant alleles alone, and other (epi)genetic factors modulate the effect of the final functional enzyme (Dipple and McCabe 2000; Sriram et al 2005).

Analysis of the homology model of human βUP, revealed that none of the mutation sites are found in or very near the active site. Instead, the two exchanges most deleterious to enzymatic activity occur at subunit surfaces that are buried upon dimerization. As a similar observation was made for previously reported point mutations of the human *UPB1* gene, it appears that proper subunit association of dimers or larger oligomers is required for full functionality of the encoded enzyme. This can most simply be explained in terms of enzyme stability. Alternatively, human βUP activity may be

affected by ligand-induced changes in the oligomerization state, as described for the rat liver enzyme and bacterial homologues (Matthews et al 1992; Thuku et al 2007; Stevenson et al 1992; Nagasawa et al 2000). However, such potential regulatory properties of human βUP remain to be further investigated.

The pyrimidine degradation pathway is also responsible for degradation of the chemotherapeutic drug, 5-fluorouracil (5-FU). It is well known that patients with either complete or partial DPD deficiency can show severe toxicity after 5-FU administration (van Kuilenburg 2004; van Kuilenburg et al 2000). Furthermore, it has been demonstrated that patients with partial DHP deficiency are prone to develop severe 5-FU toxicity (van Kuilenburg et al 2003), and heterozygous mutations in the *UPB1* gene may impair uracil catabolism (Fidlerova et al 2012; Thomas et al 2008). Therefore, risk of developing 5-FU toxicity is not limited to DPD deficiency, and patients with βUP deficiency may also be at risk of developing severe 5-FU toxicity.

Our study shows that even though the clinical manifestation of βUP deficient patients varies considerably from symptomless to severely neurologically affected, high frequency of the p.R326Q mutation in Japanese patients, and relatively high prevalence of the p.R326Q mutation in the Japanese population, suggests there may be additional undiagnosed patients with βUP deficiency. Thus, pyrimidine degradation defects should be included in differential diagnosis of unexplained neurological abnormalities, such as convulsions, developmental delay, autism and related disorders.

Conflict of interest None

References

Assmann B, Gohlich-Ratmann G, Wagner L, Moolenaar S, Engelke U, Wevers R, Voit T, Hoffmann GF (1998) Presumptive ureidopropionase deficiency as a new defect in pyrimidine catabolism found with in vitro H-NMR spectroscopy. J Inherit Metab Dis 21:Suppl 2

Assmann B, Gohlich G, Baethmann M et al (2006) Clinical findings and a therapeutic trial in the first patient with beta-ureidopropionase deficiency. Neuropediatrics 37(1):20–25

Begriche K, Massart J, Fromenty B (2010) Effects of beta-aminoisobutyric acid on leptin production and lipid homeostasis: mechanisms and possible relevance for the prevention of obesity. Fundam Clin Pharmacol 24(3):269–282

DeLano WL. 2002. The PyMOL Molecular Graphics System, DeLano Scientific, Palo Alto, CA, USA.http://www.pymol.org

Dipple KM, McCabe ER (2000) Phenotypes of patients with "simple" Mendelian disorders are complex traits: thresholds, modifiers, and systems dynamics. Am J Hum Genet 66(6):1729–1735

Emsley P, Lohkamp B, Scott WG, Cowtan K (2010) Features and development of Coot. Acta Crystallogr D Biol Crystallogr 66(Pt 4):486–501

Fidlerova J, Kleiblova P, Kormunda S, Novotny J, Kleibl Z (2012) Contribution of the beta-ureidopropionase (UPB1) gene alterations to the development of fluoropyrimidine-related toxicity. Pharmacol Rep 64(5):1234–1242

Huang M, Graves LM (2003) De novo synthesis of pyrimidine nucleotides; emerging interfaces with signal transduction pathways. Cell Mol Life Sci 60(2):321–336

Kuhara T, Ohse M, Inoue Y, Shinka T (2009) Five cases of beta-ureidopropionase deficiency detected by GC/MS analysis of urine metabolome. J Mass Spectrom 44(2):214–221

Lundgren S, Lohkamp B, Andersen B, Piskur J, Dobritzsch D (2008) The crystal structure of beta-alanine synthase from Drosophila melanogaster reveals a homooctameric helical turn-like assembly. J Mol Biol 377(5):1544–1559

Matthews MM, Liao W, Kvalnes–Krick KL, Traut TW (1992) b-Alanine synthase: purification and allosteric properties. Arch Biochem Biophys 293:254–263

Nagasawa T, Wiesner M, Nakamura T, Iwahara H, Yoshida T, Gekko K (2000) Nitrilase of Rhodococcus rhodochrous J1 - Conversion into the active form by subunit association. Eur J Biochem 267:138–144

Ohse M, Matsuo M, Ishida A, Kuhara T (2002) Screening and diagnosis of beta-ureidopropionase deficiency by gas chromatographic/mass spectrometric analysis of urine. J Mass Spectrom 37(9):954–962

Pace HC, Brenner C. (2001) The nitrilase superfamily: classification, structure and function. Genome Biol 2(1):REVIEWS0001

Schmieden V, Betz H (1995) Pharmacology of the inhibitory glycine receptor: agonist and antagonist actions of amino acids and piperidine carboxylic acid compounds. Mol Pharmacol 48(5):919–927

Signore AP, Zhang F, Weng Z, Gao Y, Chen J (2008) Leptin neuroprotection in the CNS: mechanisms and therapeutic potentials. J Neurochem 106(5):1977–1990

Sriram G, Martinez JA, McCabe ER, Liao JC, Dipple KM (2005) Single-gene disorders: what role could moonlighting enzymes play? Am J Hum Genet 76(6):911–924

Stevenson DE, Feng R, Dumas F, Groleau D, Mihoc A, Storer AC (1992) Mechanistic and structural studies on Rhodococcus ATCC 39484 nitrilase. Biotechnol Appl Biochem.15:283–302

Thomas HR, Ezzeldin HH, Guarcello V, Mattison LK, Fridley BL, Diasio RB (2008) Genetic regulation of beta-ureidopropionase and its possible implication in altered uracil catabolism. Pharmacogenet Genomics 18(1):25–35

Thuku RN, Weber BW, Varsani A, Sewell BT (2007) Post-translational cleavage of recombinantly expressed nitrilase from Rhodococcus rhodochrous J1 yields a stable, active helical form. FEBS J 274: 2099–2108

Traut TW (1994) Physiological concentrations of purines and pyrimidines. Mol Cell Biochem 140(1):1–22

van Kuilenburg ABP (2004) Dihydropyrimidine dehydrogenase and the efficacy and toxicity of 5-fluorouracil. Eur J Cancer 40(7):939–950

Van Kuilenburg ABP, Van Lenthe H, Van Gennip AH (1999) A radiochemical assay for beta-ureidopropionase using radiolabeled N-carbamyl-beta-alanine obtained via hydrolysis of [2-(14)C]5, 6-dihydrouracil. Anal Biochem 272(2):250–253

van Kuilenburg ABP, Haasjes J, Richel DJ et al (2000) Clinical implications of dihydropyrimidine dehydrogenase (DPD) deficiency in patients with severe 5-fluorouracil-associated toxicity: identification of new mutations in the DPD gene. Clin Cancer Res 6(12):4705–4712

van Kuilenburg ABP, Meinsma R, Zonnenberg BA et al (2003) Dihydropyrimidinase deficiency and severe 5-fluorouracil toxicity. Clin Cancer Res 9(12):4363–4367

van Kuilenburg ABP, Meinsma R, Beke E et al (2004a) beta-Ureidopropionase deficiency: an inborn error of pyrimidine degradation associated with neurological abnormalities. Hum Mol Genet 13(22):2793–2801

van Kuilenburg ABP, Stroomer AE, Van Lenthe H, Abeling NG, Van Gennip AH (2004b) New insights in dihydropyrimidine dehydrogenase deficiency: a pivotal role for beta-aminoisobutyric acid? Biochem J 379(Pt 1):119–124

van Kuilenburg ABP, van Lenthe H, van Cruchten A, Kulik W (2004c) Quantification of 5,6-dihydrouracil by HPLC-electrospray tandem mass spectrometry. Clin Chem 50(1):236–238

van Kuilenburg ABP, Stroomer AE, Bosch AM, Duran M (2008) Beta-alanine and beta-aminoisobutyric acid levels in two siblings with dihydropyrimidinase deficiency. Nucleosides, Nucleotides Nucleic Acids 27(6):825–829

van Kuilenburg ABP, Dobritzsch D, Meijer J et al (2012) β-Ureidopropionase deficiency: phenotype, genotype and protein structural consequences in 16 patients. Biochim Biophys Acta 1822(7):1096–1108

van Lenthe H, van Kuilenburg ABP, Ito T et al (2000) Defects in pyrimidine degradation identified by HPLC-electrospray tandem mass spectrometry of urine specimens or urine-soaked filter paper strips. Clin Chem 46(12):1916–1922

Vreken P, van Kuilenburg ABP, Hamajima N et al (1999) cDNA cloning, genomic structure and chromosomal localization of the human BUP-1 gene encoding beta-ureidopropionase. Biochim Biophys Acta 1447(2–3):251–257

Wasternack C (1980) Degradation of pyrimidines and pyrimidine analogs–pathways and mutual influences. Pharmacol Ther 8(3):629–651

Yaplito-Lee J, Pitt J, Meijer J, Zoetekouw L, Meinsma R, van Kuilenburg ABP (2008) Beta-ureidopropionase deficiency presenting with congenital anomalies of the urogenital and colorectal systems. Mol Genet Metab 93(2):190–194

Modulation of CD93 molecule in a human monocyte-like cell line (U937) treated with nickel

Nobunao IKEWAKI　Tohru SONODA*　Heihachi MIGITA**

Laboratory of Clinical Immunology, Department of Animal Pharmaceutical Science, Kyushu University of Health and Welfare
*Department of Occupational Therapy, Kyushu University of Health and Welfare
**Department of Medical Engineering, Kyushu University of Health and Welfare

ニッケルで処理されたヒト単球系細胞株(U937)におけるCD93分子の動態

池脇　信直　　園田　徹*　　右田　平八**

九州保健福祉大学　薬学部　動物生命薬科学科　臨床免疫学研究室
*九州保健福祉大学　保健科学部　作業療法学科
**九州保健福祉大学　保健科学部　臨床工学科

九州保健福祉大学　研究紀要　第15号　別刷
平成26年3月25日

Reprinted from Journal of Kyushu University of Health and Welfare
No.15　129～137　March　2014